INFLUENCE OF PARTICLE SHAPE ON THE DRAG COEFFICIENT FOR ISOMETRIC PARTICLES

Miloslav HARTMAN, Otakar TRNKA, Karel SVOBODA and Vaclav VESELY

Institute of Chemical Process Fundamentals,
Academy of Sciences of the Czech Republic, 165 02 Prague 6-Suchdol, The Czech Republic

Received May 10, 1994
Accepted August 22, 1994

A comprehensive correlation has been developed of the drag coefficient for nonspherical isometric particles as a function the Reynolds number and the particle sphericity on the basis of data reported in the literature. The proposed formula covers the Stokes, the transitional and the Newton region. The predictions of the reported correlation have been compared to experimental data measured in this work with the dolomitic materials in respect to their use in calcination and gas cleaning processes with fluidized beds. Approximative explicit formulae have also been reported that make it possible to estimate the terminal free-fall velocity of a given particle or to predict the particle diameter corresponding to a fluid velocity of interest.

Sulfur dioxide as well as other acidic gaseous pollutants (e.g., hydrogen chloride and hydrogen fluoride) can be controlled by means of alkaline earth oxides, hydroxides or carbonates[1]. Whereas previous investigations have mostly been confined to calcium-based sorbents (calcium quicklime, calcium hydrate), the use of dolomitic materials (dolomitic quicklime, dolomitic hydrate) is a more practical expedient for once-through technologies. In difference to the limestone-based materials, there is very little information available on the dolomite-derived solids.

Harmful gaseous pollutants are removed by the entrained sorbent particles in the duct, the transport-line reactor or in the circulating fluidized bed or by passing through the bubbling fluidized bed of sorbent[2–4]. Under the operation conditions usually found in the cleaning processes, the precursor particles (carbonate, hydroxide) decompose first forming particles of the corresponding metal oxides[5,6] which subsequently react with the gaseous species.

In addition to the above situations, the needs frequently occur in other engineering problems to deal with the motion of solid particles in fluids. The terminal velocities of isolated particles free-falling in an infinite fluid are needed in cyclone design, classification, crystallization and in fluidized bed processes. As our recent comprehensive reviews[7,8] indicate, the terminal velocity of spherical particles falling in an infinite Newtonian fluid as well as the minimum fluidization velocity can accurately be predicted. Reliable correlations are available in the literature[9,10] relating the drag coefficient C_D to the Reynolds number of spheres falling at their terminal velocities. Several interpolation formulae of various form have also been developed[11–15]. Such explicit relationships make it possible to eliminate the common need for an iterative solution specifying the free fall conditions of spherical particles.

In contrast to spheres, little is known about the terminal velocity and settling characteristics of irregular particles in fluids. This dearth of knowledge results mainly from a fact that the drag on nonspherical particles is strongly dependent on their shape, and because the shape cannot be simply or precisely described, even with the use of current advanced techniques. Different approaches to the free settling of nonspherical bodies can be found in the literature[16–20].

This communication is a sequel to a previous work of ours[21] on the rate of steady-state motion of isomeric bodies (glass spheres, particles of limestone and lime) in an infinite fluid. The objective of the present investigation is to provide the data on dolomitic materials as well as develop alternative relationships for estimating the settling rates of nonspherical, isomeric particles.

THEORETICAL

When a particle moves through a fluid, there exists a resisting force called drag which is dependent on the particle size, particle shape, an adequately defined area, relative velocity and the density and the viscosity of the fluid. A dimensionless parameter, called the drag coefficient, C_D, is defined (see Eq. (*1*)) as the ratio of the drag force to the inertial forces,

$$C_D\, Re_t^2 = \frac{4}{3} Ar \quad . \tag{1}$$

The sphericity, ψ, is usually employed as the single measure to account for particle shape. It is introduced as the ratio

$$\psi = \text{surface area of sphere/surface area of particle} \tag{2}$$

at the same volume.

Thus, $\psi = 1$ for perfect spheres and $0 < \psi < 1$ for other bodies.

However, the sphericity is a theoretical concept which can be realized only imperfectly. There is no simple generally accepted method for measuring the sphericity of smaller irregular particles. Fractal studies[20,22] suggest that the surface area of many real particles is generally indeterminate and is influenced by the technique with which it is measured. It should be noted that the sphericity used in this work follows the packed bed/Ergun approach[23–25]. For the sphericity of some regular bodies as well as for the sphericity of a number of common materials, the reader is referred to the data tabulated in the review[8].

A host of measures have been proposed for the size of nonspherical particles. As a practical means, the equivalent spherical diameter, d_{sph}, based on the same volume has usually been employed. For isometric particles, the equivalent spherical diameter can be approximated by the screen size:

$$d_{\mathrm{sph}} \approx d_{\mathrm{scr}} = d_{\mathrm{p}} \quad . \tag{3}$$

The particle size defined in this manner has been used in this study.

Development of a Correlation of the Drag Coefficient for Nonspherical Isometric Particles

The experimental data amassed by Pettyjohn and Christiansen[16] have been employed in this study. Working with well-defined bodies, the authors[16] determined by experiment the settling velocities of the following isometric shapes: spheres ($\psi = 1$; 30 data points; Re_t ε <0.0359, 22 640>), cube octahedrons ($\psi = 0.906$; 130 data points; Re_t ε <0.00592, 17 410>), octahedrons ($\psi = 0.846$; 80 data points; Re_t ε <0.00837, 17 350), cubes ($\psi = 0.806$; 135 data points; Re_t ε <0.0076, 16 080>) and tetrahedrons ($\psi = 0.670$; 65 data points; Re_t ε <0.00691, 13 310>). Settling rates were observed with white mineral oil, water and water–glucose solutions in a 0.5 m × 0.5 m square settling column and in a 0.2 m i.d, glass tube.

The results of Turton and Levenspiel[9] and Haider and Levenspiel[19] indicate that various experimental data on free settling of particles can be fitted by a five-parameter relationship

$$C_D\,(Re_{\mathrm{t}},\psi) = \frac{24}{Re_{\mathrm{t}}}\left(1 + k_1\,Re_{\mathrm{t}}^{k_2}\right) + \frac{k_3}{1 + k_4\,Re_{\mathrm{t}}^{k_5}} \quad . \tag{4}$$

Using Eq. (*4*) we have searched for the values of $k_1 - k_5$ so as to minimize the sum of squared errors, Q, defined by

$$Q = \sum_{i=1}^{n} (\log_{10} C_{D,\mathrm{exp}} - \log_{10} C_{D,\mathrm{calc}})^2 \quad . \tag{5}$$

This was performed with the aid of a flexible polyhedron search, also called the simplex minimization. The resulting parameters $k_1 - k_5$ for the respective sphericities are given in Table I. Quality of the fit is documented using the standard deviation, s, as a statistical measure

$$s = (Q/n)^{1/2} \quad . \tag{6}$$

As can be seen from the values of s given in Table I, the five-constant equation (*4*) describes the experimental data quite well. This Table also shows that the parameters $k_1 - k_5$ are functions of the shape. Once such functions are established, it would make it possible to interpolate for different sphericities of interest.

Optimization runs also indicated that there existed a dependence between the coefficients k_4 and k_5. Therefore, an average, constant value of $\overline{k}_5 = -1.26$ was employed in further search of $C_D = C_D\,(Re_t, \psi)$. Then, the respective parameters, $k_1 - k_4$ were established as functions of sphericity as follows:

$$k_1 = 2.9245 \exp\,(-2.8416\,\psi) \tag{7}$$

$$k_2 = 0.20477 + 0.45060\,\psi \tag{8}$$

TABLE I
Fitted parameters in the correlation (*4*) for bodies of different shape, evaluated on the basis of the experimental results reported by Pettyjohn and Christiansen[16]

Parameter	Sphericity, ψ				
	1[a]	0.906	0.846	0.806	0.670
k_1	0.173	0.224	0.264	0.287	0.425
k_2	0.657	0.609	0.597	0.561	0.540
k_3	0.413	0.763	1.139	1.334	1.829
k_4	16 300	7 843	9 369	2 652	1 556
k_5	–1.09	–1.30	–1.31	–1.20	–1.38
Standard deviation, s	0.020	0.021	0.024	0.025	0.037

[a] Cofficients for spheres (ψ = 1) are taken from the work of Turton and Levenspiel[9]. The values are based on more than four hundred experimental data points reported by different investigators for spheres.

$$k_3 = 5.0178 - 4.6404\,\psi \qquad (9)$$

$$k_4 = 0.60430\,\exp\,(10.9399\,\psi) \qquad (10)$$

$$k_5 \equiv \overline{k}_5 = -1.26 \qquad (11)$$

for $\psi > 0.67$.

It is of importance that on introducing Eqs (*7*) – (*11*) into Eq. (*4*), the increase of the standard deviation, *s*, was practically negligible. Of course, the final empirical correlation developed here, and embodied in Eqs (*4*) and (*7*) – (*11*), has usual limitations. It should be applied with caution outside the experimental conditions from which it was educed. We believe that the extrapolation to about $\psi = 0.5$ may be feasible.

For illustration, the drag coefficient, C_D, has been computed for different Re_t and ψ from Eqs (*4*) and (*7*) – (*11*). The results are plotted in Fig. 1 and they show that the proposed five-constant correlation is capable of describing a minimum on the curves C_D vs Re_t for all the employed shapes. As evident, particles exhibite higher drag as they become less spherical.

An alternative illustration of the function $C_D = C_D\,(\psi, Re_t)$ is presented in Fig. 2 for two values of *Ar* (500 and 10^4) which approximately outline the range of experiments carried out in this work.

Since Re_t occurs in both Eq. (*1*) and Eq. (*4*), an adequate iteration technique is needed to estimate the terminal velocity of a given spherical or nonspherical particle. In

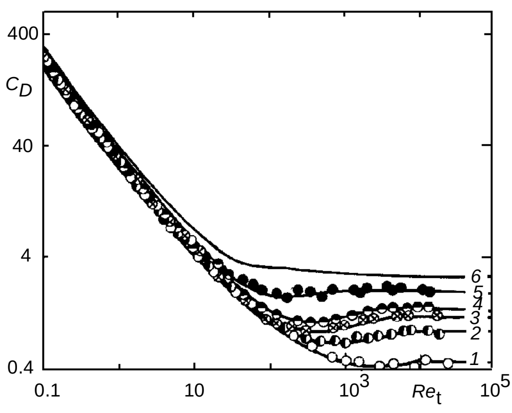

FIG. 1
Drag coefficient as a function of the Reynolds number and the sphericity; experimental data points are results reported by Pettyjohn and Christiansen[16], the solid lines show the drag coefficient predicted from the correlation embodied in Eqs (*4*), (*7*) – (*11*) for the respective shapes: *1* , $\psi = 1$; *2* , $\psi = 0.906$; *3* , $\psi = 0.846$; *4* , $\psi = 0.806$; *5* , $\psi = 0.67$; *6* , $\psi = 0.5$ (extrapolation)

design, a situation also frequently occurs when the diameter of particles, that are just entrained under certain operation conditions, is to be predicted. For such cases it is practical to rewrite Eq. (*1*) as

$$Re_t = C_D\,(Re_t,\psi)/Y\ , \tag{12}$$

where Y is the dimensionless group defined by

$$Y = 4\boldsymbol{g}(\rho_s - \rho_f)\,\mu_f/(3U_t^3\rho_f^2)\ . \tag{13}$$

As can be seen, the diameter of particle does not occur in the quantity *Y*. To find the particle size corresponding to a terminal velocity of interest, an iterative solution of Eq. (*12*) together with the expression for $C_D = C_D\ (Re_t,\ \psi)$ must be sought. Elementary procedure such as interval halving has proven to be effective.

Using the proposed correlation given by Eqs (*4*) and (*7*) – (*11*) we have made systematic predictions of the free-fall conditions from Eq. (*1*) for selected values of the Archimedes number ($Ar\ \varepsilon$ <1, 5 . 10^7>) and the sphericity (ψ = 1, 0.8 and 0.5). The estimated values of Re_t, *Y* and C_D are given in Table II. Our experience indicates that such tabulated results are helpful in quick solving many engineering problems in which various free-fall situations occur with nonspherical particles.

Some of the predictions of Eqs (*4*) and (*7*) – (*11*) will be compared in the following part of the paper to new experimental results measured with crushed particles of dolomite and dolomitic lime.

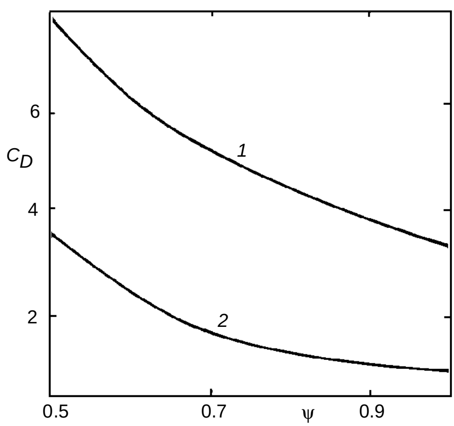

FIG. 2
Dependence of the drag coefficient of a particle on its sphericity predicted from Eqs (*4*) and (*7*) – (*11*): *1* *Ar* = 500 (Re_t = 9.4 – 14.1), *2* *Ar* = 10 000 (Re_t = 61.6 – 115)

TABLE II
Steady-state free-fall conditions estimated from Eqs (*1*), (*4*), (*7*) – (*11*) for isometric particles of different shape

Ar	ψ = 1			ψ = 0.8			ψ = 0.5		
	Re_t	Y	C_D	Re_t	Y	C_D	Re_t	Y	C_D
1E 00	5.42E–02	8.38E 03	4.54E 02	5.26E–02	9.18E 03	4.83E 02	4.67E–02	1.31E 04	6.11E 02
5E 00	2.59E–01	3.82E 02	9.90E 01	2.45E–01	4.56E 02	1.11E 02	2.05E–01	7.77E 02	1.59E 02
1E 01	5.01E–01	1.06E 02	5.31E 01	4.65E–01	1.33E 02	6.17E 01	3.79E–01	2.45E 02	9.28E 01
5E 01	2.16E 00	6.57E 00	1.42E 01	1.93 E 00	9.23E 00	1.78E 01	1.51E 00	1.95E 01	2.94E 01
1E 02	3.92E 00	2.22E 00	8.68E 00	3.46E 00	3.23E 00	1.12E 01	2.67E 00	7.04E 00	1.88E 01
5E 02	1.41E 01	2.37E–01	3.34E 00	1.23E 01	3.55E–01	4.38E 00	9.38E 00	8.07E–01	7.57E 00
1E 03	2.36E 01	1.02E–01	2.40E 00	2.07E 01	1.50E 01	3.11E 00	1.54E 01	3.63E–01	5.61E 00
5E 03	7.25E 01	1.75E–02	1.27E 00	6.42E 01	2.52E–02	1.62E 00	4.21E 01	8.93E–02	3.76E 00
1E 04	1.15E 02	8.82E–03	1.01E 00	1.01E 02	1.31E–02	1.32E 00	6.16E 01	5.69E–02	3.51E 00
5E 04	3.20E 02	2.03E–03	6.51E–01	2.54E 02	4.06E–03	1.03E 00	1.42E 02	2.31E–02	3.28E 00
1E 05	4.88E 02	1.15E–03	5.59E–01	3.61E 02	2.83E–03	1.02E 00	2.03E 02	1.59E–02	3.23E 00
5E 05	1.23E 03	3.61E–04	4.43E–01	7.69E 02	1.46E–03	1.13E 00	4.64E 02	6.69E–03	3.10E 00
1E 06	1.77E 03	2.40E–04	4.25E–01	1.06E 03	1.13E–03	1.19E 00	6.61E 02	4.61E–03	3.05E 00
5E 06	3.94E 03	1.09E–04	4.30E–01	2.24E 03	5.91E–04	1.33E 00	1.51E 03	1.95E–03	2.94E 00
1E 07	5.49E 03	8.05E–05	4.42E–01	3.13E 03	4.35E–04	1.36E 00	2.14E 03	1.35E–03	2.30E 00
5E 07	1.20E 04	3.89E–05	4.65E–01	6.91E 03	2.02E–04	1.40E 00	4.86E 03	5.83E–04	2.83E 00

EXPERIMENTAL

The terminal velocities of narrow fractions of dolomite and dolomitic lime particles determined from the dependence of pressure drop vs gas velocity for a shallow bed of such particles were measured in a fluidization column[25]. A glass column of inside diameter 0.085 m and height 2 m was employed. The flow rate of air was gradually increased and pressure drop of fluidized bed vs the superficial velocity of air was recorded. The terminal velocities reported in this study are the arithmetic mean of the velocity at which the decline in pressure drop becomes noticeable and that when practically all the particles are entrained out of the column. These values are related to the mean sieve size of the particles. As can be seen, the free fall of a particle through a static gas and moving the gas upwards past the particle at the same relative velocity are not the identical situations. Such phenomena as a velocity distribution across the column and random velocity fluctuations with respect to time may become more or less significant in the latter process.

The difference between the start and the end of elutriation depends upon the width of a collected fraction (0.025 – 0.13 mm). It increases from about 0.05 m s^{-1} for the smallest particles to about 0.25 m s^{-1} for the largest ones. Three to five replicate runs with the respective fractions showed reproducibility of the terminal velocity better than 5%. Their values varied from 0.45 to 2.70 m s^{-1} for the dolomite particles and from 0.40 to 2.48 m s^{-1} for the calcined particles.

The measurements were conducted under ambient conditions (ρ_{air} = 1.200 kg m^{-3}, μ_{air} = 1.81 . 10^{-5} Pa s) with a dolomite and its calcine. The particles comprised five narrow, carefully sieved fractions: 0.100 to 0.125 mm ($\bar{d}_p$ = 0.112 mm), 0.20 to 0.25 mm ($\bar{d}_p$ = 0.225 mm), 0.25 to 0.315 mm ($\bar{d}_p$ = 0.282 mm), 0.40 to 0.50 mm ($\bar{d}_p$ = 0.450 mm) and 0.50 to 0.63 mm ($\bar{d}_p$ = 0.565 mm). The measured bulk density of the dolomite and dolomitic lime particles amounted to 2 650 and 1 550 kg m^{-3}, respectively. Particle sphericity was determined by a procedure based on pressure drop measurements of the fixed (packed, static) bed[23,26]. Repeated measurements provided the averaged values of sphericity ψ = 0.6 (0.54 – 0.66) for dolomite and ψ = 0.8 (0.75 – 0.85) for dolomitic lime.

RESULTS AND DISCUSSION

The measurements of the terminal velocity of nonspherical, isometric particles have been interpreted in terms of the drag coefficient and the Reynolds number corresponding to the terminal velocity measured. These quantities for the five fractions of dolomite particles are plotted in Fig. 3. As can be seen the curve computed from Eqs (*4*) and (*7*) – (*11*) follows reasonably the trend indicated by the experimental data points. The largest difference between the experimental and predicted values amounts to about 30%. However, one should realize that with respect to Eq. (*1*), a given inaccuracy in the Reynolds number results in a doublefold error in the drag coefficient. Possible effects of the superficial gas velocity profile developed within the fluidization column as well as velocity fluctuations cannot also be overlooked. We believe that the results plotted in Fig. 3 as well as those in Fig. 4 demonstrate reasonable agreement between predicted and experimental data on the drag coefficient for the nonspherical particles of dolomitic materials.

Making use of the asymptotic expressions[27] for Re_t at very low and very high Reynolds numbers leads to an explicit relationship between Re_t and Y for different ψ

$$Re_t\,(Y,\psi) = \frac{C'_D}{Y}\left[1 + \left(\frac{4.899}{C'_D\,K^{0.5}}\right)^{1.351} . \, Y^{\,0.6755}\right]^{0.7402} . \qquad (14)$$

The quantities C'_D and K can be taken from the work of Pettyjohn and Christiansen[16] for ψ ε <0.67, 1> as

$$K = 0.843 \log_{10}(\psi/0.065)\ , \qquad (15)$$

and

$$C'_D = 5.31 - 4.88\psi\ . \qquad (16)$$

Experience indicates, that the simplified Eqs (*14*) – (*16*) provide predictions of Re_t as a function of Y about 5 – 15% higher than those obtained from more rigorous Eqs (*4*), (*7*) – (*12*).

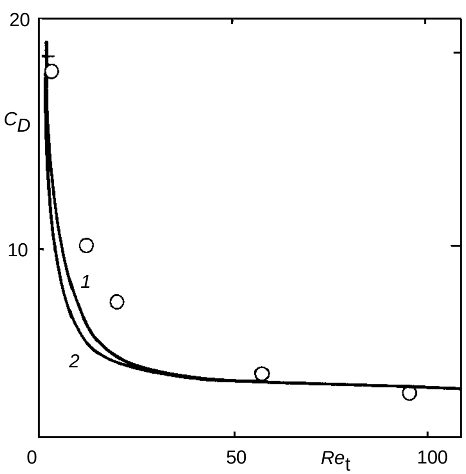

FIG. 3
Comparison of the experimental and predicted values of the drag coefficient for the particles of crushed dolomite (ψ = 0.6); ❍ experimental data. Curve *1* depicts the drag coefficient predicted by Eqs (*4*) and (*7*) – (*11*); curve *2* depicts the drag coefficient predicted with the use of Eqs (*14*) – (*16*)

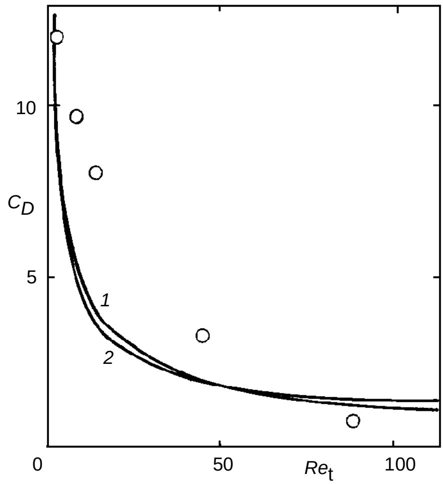

FIG. 4
Comparison of the experimental and predicted values of the drag coefficient for the particles of dolomitic lime (ψ = 0.8): ❍ experimental data. Curve *1* depicts the drag coefficient predicted by Eqs (*4*) and (*7*) – (*11*); curve *2* depicts the drag coefficient predicted with the use of Eq. (*20*)

Using an approach similar to that of Churchill and Usagi[27], Haider and Levenspiel[19] proposed the following explicit relation between the dimensionless terminal velocity of a particle, U_t^*, and its dimensionless diameter, d^*, and sphericity, ψ:

$$U_t^* = \left[\frac{18}{{d^*}^2} + \frac{2.335 - 1.744\,\psi}{{d^*}^{0.5}}\right]^{-1} \qquad (17)$$

for ψ ε <0.5, 1>.

With the use of the Reynolds and Archimedes numbers as variables

$$U_t^* = Re_t/Ar^{1/3} \qquad (18)$$

$$d^* = Ar^{1/3} \qquad (19)$$

the Haider and Levenspiel equation can be recast into the form

$$Re_t = \frac{Ar}{18 + (2.335 - 1.744\,\psi)\,Ar^{1/2}} \quad . \qquad (20)$$

The explicit relationships (*14*) and (*20*) can be viewed as practical simplified approximations to rigorous Eqs (*1*), (*4*), (*7*) – (*12*). On the other hand, the use of Eqs (*14*) and (*20*) eliminates the need for the iterative computations. The confrontations of Eqs (*14*) and (*20*) with the iterative solutions shown in Figs 3 and 4 indicate that the differences are less than 15%.

CONCLUSIONS

The presented relationships provide a well-founded possibility for predicting the steady-state, free-fall conditions of nonspherical, isometric particles.

The results of elutriation experiments obtained with the dolomitic materials can readily by employed in design and development of the calcination and gas cleaning processes with a gas–solid contacting mode of interest.

The authors acknowledge the financial support extended by the Grant Agency of the Czech Republic (Grant No. 203/94/0111) and the Grant Agency of the Academy of Sciences of the Czech Republic (Grant No. 472113).

SYMBOLS

Ar	Archimedes number, $Ar = d_p^3 \boldsymbol{g} \rho_f (\rho_s - \rho_f) / \mu_f^2$
C_D	drag coefficient of particle, $C_D = 4\boldsymbol{g} d_p (\rho_s - \rho_f) / (3U_t^2 \rho_f)$
$C_{D,\mathrm{exp}}$	drag coefficient determined by experiment
$C_{D,\mathrm{calc}}$	drag coefficient calculated
C_D'	quantity defined by Eq. (*16*)
d_p	diameter of particles, m
$\bar{d}_p$	mean diameter of particles, m
d_{scr}	screen size of particles, m
d_{sph}	equivalent spherical diameter or diameter of a sphere which has the same volume as the particle, m
d^*	dimensionless particle diameter, $d^* = Ar^{1/3} = (3\, C_D\, Re_t^2/4)^{1/3}$
$\boldsymbol{g}$	acceleration due to gravity, $\boldsymbol{g}$ = 9.807 m s^{-2}
$k_1 - k_5$	fitted constants in Eq. (*4*)
K	quantity defined by Eq. (*15*)
n	number of data points in evaluating constants
Q	sum of squared errors defined in Eq. (*5*)
Re_t	Reynolds number at terminal velocity of falling particle, $Re_t = U_t\, d_p\, \rho_f / \mu_f$
s	standard deviation defined in Eq. (*6*)
U_t	terminal, free fall velocity of particle, m s^{-1}
U_t^*	dimensionless terminal velocity of particle, $U_t^* = Re_t / Ar^{1/3} = U_t\, [\rho_f^2 / (\boldsymbol{g}\, \mu_f\, (\rho_s - \rho_f))]^{1/3}$
Y	dimensionless group, $Y = 4\boldsymbol{g}\, (\rho_s - \rho_f)\, \mu_f / (3\, U_t^3 \rho_f^2) = 4\, Ar/(3\, Re_t^3) = C_D/Re_t$
μ_f	fluid viscosity, Pa s
ρ_f	fluid density, kg m^{-3}
ρ_s	particle density (bulk), kg m^{-3}
ψ	particle sphericity, shape factor

REFERENCES

1. Hartman M., Pata J.: Int. Chem. Eng. *18*, 712 (1978).
2. Hartman M., Svoboda K., Trnka O., Coughlin R. W.: Ind. Eng. Chem., Process Des. Dev. *22*, 598 (1983).
3. Hartman M., Svoboda K., Trnka O., Vesely V.: Chem. Eng. Sci. *43*, 2045 (1988).
4. Hartman M., Svoboda K., Trnka O.: Ind. Eng. Chem. Res. *30*, 1855 (1991).
5. Hartman M., Trnka O., Vesely V.: AIChE J. *40*, 536 (1994).
6. Hartman M., Trnka O., Svoboda K., Kocurek J.: Chem. Eng. Sci. *49*, 1209 (1994).
7. Hartman M., Yates J. G.: Collect. Czech. Chem. Commun. *58*, 961 (1993).
8. Hartman M., Coughlin R. W.: Collect. Czech. Chem. Commun. *58*, 1213 (1993).
9. Turton R., Levenspiel O.: Powder Technol. *47*, 83 (1986).
10. Flemmer R. L. C., Banks C. L.: Powder Technol. *48*, 217 (1986).
11. Zigrang D. J., Sylvester N. D.: AIChE J. *27*, 1043 (1981).
12. Turton R., Clark N. N.: Powder Technol. *53*, 127 (1987).
13. Wesselingh J. A.: Chem. Eng. Process. *27*, 9 (1987).
14. Hartman M., Havlin V., Trnka O., Carsky M.: Chem. Eng. Sci. *44*, 1743 (1989).
15. Hartman M., Vesely V., Svoboda K., Havlin V.: Collect. Czech. Chem. Commun. *55*, 403 (1990).
16. Pettyjohn E. S., Christiansen E. B.: Chem. Eng. Prog. *44* (2), 157 (1948).

17. Becker H. A.: Can. J. Chem. Eng. *37*, 85 (1959).
18. Christiansen E. B., Barker D. H.: AIChE J. *11*, 145 (1965).
19. Haider A., Levenspiel O.: Powder Technol. *58*, 63 (1989).
20. Clark N. N., Gabriele P., Shuker S., Turton R.: Powder Technol. *59*, 69 (1989).
21. Hartman M., Trnka O., Svoboda K.: Ind. Eng. Chem. Res. *33*, 1979 (1994).
22. Mandelbrot B. B.: *Form, Chance, and Dimension.* Freeman, San Francisco 1977.
23. Svoboda K., Hartman M.: Ind. Eng. Chem., Process Des. Dev. *20*, 319 (1981).
24. Yates J. G.: *Fundamentals of Fluidized-Bed Chemical Processes*, p. 8. Butterworths, London 1983.
25. Kunii D., Levenspiel O.: *Fluidization Engineering*, 2nd ed., p. 64. Butterworth–Heinemann, Boston 1991.
26. Hartman M., Svoboda K., Vesely V.: Chem. Listy *79*, 247 (1985).
27. Churchill S. W., Usagi R.: AIChE J. *18*, 1121 (1972).

Translated by the author (M. H.).